Aromatic Amino Acids Required for Pili Conductivity and Long-Range Extracellular Electron Transport in *Geobacter sulfurreducens*

Madeline Vargas,[a,b] Nikhil S. Malvankar,[a] Pier-Luc Tremblay,[a] Ching Leang,[a] Jessica A. Smith,[a] Pranav Patel,[a] Oona Synoeyenbos-West,[a] Kelly P. Nevin,[a] Derek R. Lovley[a]

Department of Microbiology, University of Massachusetts, Amherst, Massachusetts, USA[a]; Department of Biology, College of the Holy Cross, Worcester, Massachusetts, USA[b]

ABSTRACT **It has been proposed that *Geobacter sulfurreducens* requires conductive pili for long-range electron transport to Fe(III) oxides and for high-density current production in microbial fuel cells. In order to investigate this further, we constructed a strain of *G. sulfurreducens*, designated Aro-5, which produced pili with diminished conductivity. This was accomplished by modifying the amino acid sequence of PilA, the structural pilin protein. An alanine was substituted for each of the five aromatic amino acids in the carboxyl terminus of PilA, the region in which *G. sulfurreducens* PilA differs most significantly from the PilAs of microorganisms incapable of long-range extracellular electron transport. Strain Aro-5 produced pili that were properly decorated with the multiheme *c*-type cytochrome OmcS, which is essential for Fe(III) oxide reduction. However, pili preparations of the Aro-5 strain had greatly diminished conductivity and Aro-5 cultures were severely limited in their capacity to reduce Fe(III) compared to the control strain. Current production of the Aro-5 strain, with a graphite anode serving as the electron acceptor, was less than 10% of that of the control strain. The conductivity of the Aro-5 biofilms was 10-fold lower than the control strain's. These results demonstrate that the pili of *G. sulfurreducens* must be conductive in order for the cells to be effective in extracellular long-range electron transport.**

IMPORTANCE **Extracellular electron transfer by *Geobacter* species plays an important role in the biogeochemistry of soils and sediments and has a number of bioenergy applications. For example, microbial reduction of Fe(III) oxide is one of the most geochemically significant processes in anaerobic soils, aquatic sediments, and aquifers, and *Geobacter* organisms are often abundant in such environments. *Geobacter sulfurreducens* produces the highest current densities of any known pure culture, and close relatives are often the most abundant organisms colonizing anodes in microbial fuel cells that harvest electricity from wastewater or aquatic sediments. The finding that a strain of *G. sulfurreducens* that produces pili with low conductivity is limited in these extracellular electron transport functions provides further insight into these environmentally significant processes.**

Received 12 February 2013 **Accepted** 13 February 2013 **Published** 12 March 2013

Citation Vargas M, Malvankar NS, Tremblay P-L, Leang C, Smith JA, Patel P, Synoeyenbos-West O, Nevin KP, Lovley DR. 2013. Aromatic amino acids required for pili conductivity and long-range extracellular electron transport in *Geobacter sulfurreducens*. mBio 4(2):e00105-13. doi:10.1128/mBio.00105-13.

Editor Stephen Giovannoni, Oregon State University

Address correspondence to Derek R. Lovley, dlovley@microbio.umass.edu.

The mechanisms for long-range extracellular electron transport in *Geobacter* species are of interest because of the important role that *Geobacter* species play in the biogeochemistry of a diversity of anaerobic soils and sediments and in several bioenergy strategies. For example, *Geobacter* species are frequently the most abundant Fe(III)-reducing microorganisms in soils and sediments in which Fe(III) reduction is an important process (1), influencing the cycling not only of carbon and iron but also of trace metals, metalloids, and phosphates that adsorb to Fe(III) oxides (2, 3). Anaerobic oxidation of organic contaminants coupled with the reduction of Fe(III) and reductive precipitation of contaminant metals is an important bioremediation function of *Geobacter* species (1). The ability of *Geobacter* species to make electrical connections with electrodes offers the possibility of harvesting electricity from waste organic matter or driving anaerobic processes, such as reductive dechlorination, with electrical energy (4, 5). *Geobacter* species can also make electrical connections with other species (6), which may be an important component of anaerobic degradation of organic wastes to methane (7).

Geobacter species must directly contact Fe(III) oxides in order to reduce them (8). Studies with *Geobacter sulfurreducens* have identified two components on the outer surface that are essential for Fe(III) oxide reduction, type IV pili and the multiheme *c*-type cytochrome, OmcS, which is associated with the pili (9). The pili are electrically conductive (10, 11). The spacing of OmcS molecules along the pili is too great for OmcS-to-OmcS electron transfer along the pili (12, 13). A possible explanation for these observations is that the role of the pili is to deliver electrons to OmcS at a distance from the cell, which then transfers electrons to Fe(III) oxide (4, 9).

Studies with a strain of *G. sulfurreducens* in which the gene for PilA, the structural pilus gene, was deleted have demonstrated that cells in contact with graphite electrodes can transfer electrons to electrodes in the absence of pili (14–16), but the ability to produce pili is required for *G. sulfurreducens* to develop thick, conductive

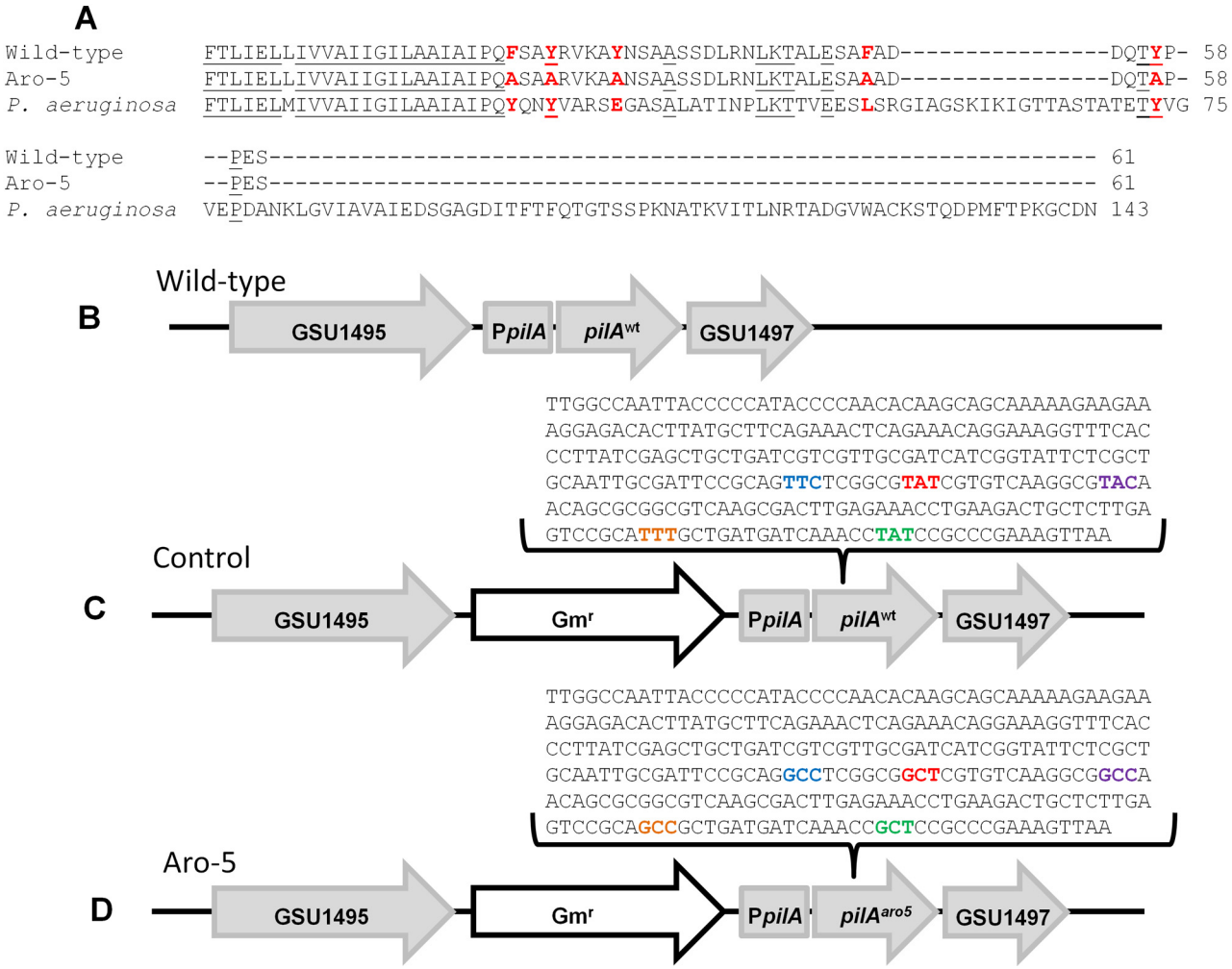

FIG 1 Alignment of amino acid sequences and genetic map. (A) Alignment of PilA of wild-type *G. sulfurreducens*, the *G. sulfurreducens* Aro-5 strain, and *Pseudomonas aeruginosa* PAO1. The alignment begins at the PilD cleavage site (34). The full PilA sequence of *G. sulfurreducens* encodes 29 amino acids prior to the cleavage site. Substituted amino acids in the PilA protein of the Aro-5 strain are in red. Amino acids that are identical between wild-type *G. sulfurreducens* and *P. aeruginosa* PAO1 are underlined. The alignment was made with ClustalW2. (B) *pilA* region of the wild-type strain. (C) *pilA* region of the control strain, encoding PilA^{wt}, which contains the wild-type sequence. (D) *pilA* region of the Aro-5 strain, encoding PilA^{Aro-5}, with codons for alanine substituted for codons for aromatic amino acids.

biofilms (14, 15) in which cells at a distance (>50 μm) from the electrode can contribute to current production (17, 18). Competing explanations for the requirement for pili include the possibilities that (i) the pili serve as a scaffold to support cytochromes involved in electron transport through the biofilm (19) and (ii) long-range electron transport through the biofilms is through the pili (20).

These models for long-range electron transport to Fe(III) and through conductive biofilms could be better evaluated if it was possible to produce a strain of *G. sulfurreducens* which could produce pili that serve as a cytochrome scaffold but have diminished conductivity. Several lines of evidence suggest that *G. sulfurreducens* pili have a metallic-like conductivity similar to that of synthetic organic metals, which might be attributed to overlapping pi-pi orbitals of aromatic constituents (11).

Aromatic amino acids are the most likely source of pi orbital stacking in a protein filament such as pili. The PilA sequences of *G. sulfurreducens* and organisms that are not capable of long-range electron transport, such as *Pseudomonas*, *Neisseria*, and *Vibrio* species, have highly conserved N-terminal sequences (10). This N-terminal domain forms an α-helix that allows monomers to interact with each other to generate a hydrophobic filament core (21). However, the *G. sulfurreducens* carboxyl terminus of the PilA sequence is truncated (Fig. 1A). Therefore, we hypothesized that aromatic amino acid moieties in this region of PilA in which *G. sulfurreducens* was atypical were potential candidates to confer the observed metallic-like conductivity via overlapping pi-pi orbitals. Here we report on the extracellular electron transfer phenotypes of a strain of *G. sulfurreducens* in which alanine was substituted for the five aromatic amino acids in the carboxyl region of PilA.

RESULTS AND DISCUSSION

We constructed a strain of *G. sulfurreducens*, designated Aro-5, in which an alanine was substituted for each of the five aromatic amino acids in the carboxyl terminus of PilA (Fig. 1). A control strain was constructed by the same approach but retained the PilA

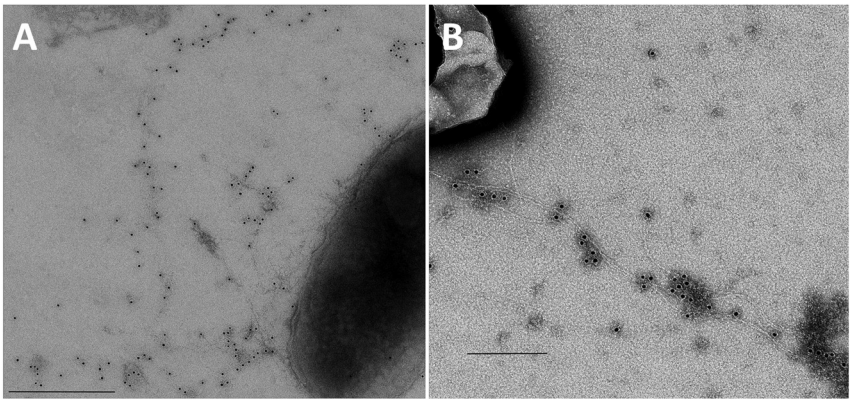

FIG 2 Transmission electron micrographs of the negatively stained Aro-5 strain grown in medium with acetate as the electron donor and fumarate as the electron acceptor and then successively labeled with anti-OmcS rabbit polyclonal antibodies and anti-rabbit IgG conjugated with secondary-antibody-labeled 10-nm gold particles. Scale bars represent 500 nm (A) and 200 nm (B).

sequence of the wild-type strain (Fig. 1). Both the Aro-5 and the control strain actively expressed *pilA*, with transcript abundances somewhat higher (2.3-to 3.0-fold; $n = 3$) in the Aro-5 strain. Transmission electron microscopy coupled with immunogold labeling revealed that the Aro-5 strain produced pili decorated with the *c*-type cytochrome OmcS (Fig. 2), similar to pili previously reported for wild-type cells (12), as did the control strain (not shown).

Measurements of the conductivity of filament preparations sheared from the outer cell surface can exhibit substantial variability between preparations from replicate cultures (11). However, conductivities of preparations from the Aro-5 strain were consistently low compared to those of the control strain (Fig. 3), which had conductivities comparable to those previously reported for the wild type (11).

In order to evaluate the impact of diminished pili conductivity on extracellular electron transfer, the Aro-5 and control strains were inoculated into medium with acetate as the sole electron donor and Fe(III) oxide as the electron acceptor. The control strain readily reduced Fe(III) oxide, but the Aro-5 strain did not (Fig. 4). These results demonstrated that pili with associated OmcS is not sufficient for effective Fe(III) oxide reduction; the pili must also be conductive.

The Aro-5 strain also appeared to be impaired in long-range electron transport through current-producing biofilms. When grown in a bioelectrochemical system with acetate as the sole electron donor and a graphite electrode as the sole electron acceptor, the control strain produced current at levels comparable to those previously reported (14) for the wild type, but the current production of the Aro-5 strain was low, comparable to that previously reported (14, 15) for a strain in which *pilA* had been deleted (Fig. 5). The primary difference between the Aro-5 anode biofilm and previously described anode biofilms of the *pilA*-deficient mutant was that the Aro-5 biofilm was as thick as that of the control strain (Fig. 6), whereas the *pilA*-deficient mutant produces thinner biofilms (14, 15). This difference may be due to the presence of pili in the Aro-5 strain, supporting better cell cohesion.

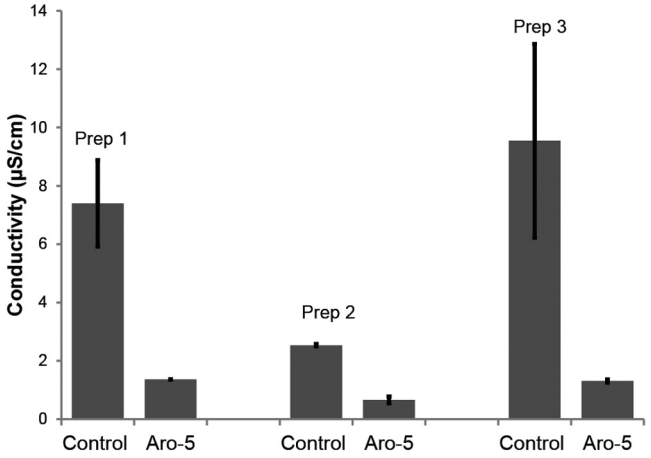

FIG 3 Conductivity of filament preparations (Prep) of the Aro-5 and control strains. Vertical bars represent the results of separate biological replicates in which an Aro-5 and a control culture were simultaneously processed. Error bars represent the means and standard deviations of triplicate measurements of each biological replicate. The difference in the conductivities of the control and Aro-5 preparations is statistically significant ($P < 0.05$, *t* test).

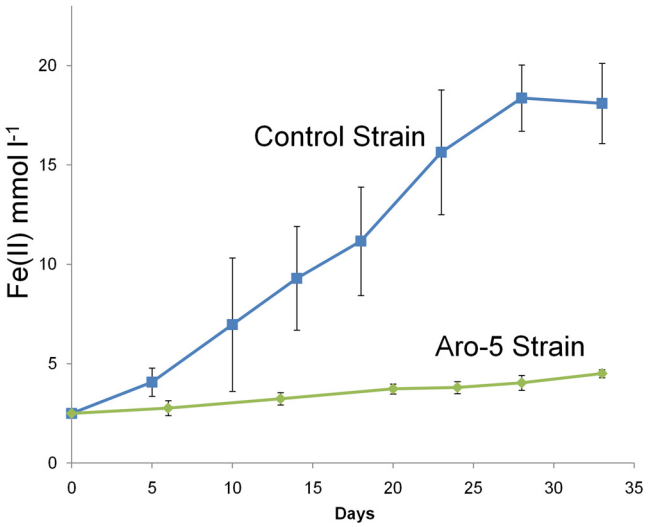

FIG 4 Fe(II) produced from Fe(III) oxide reduction over time in the Aro-5 and control strains. Results are the means and standard deviations of results from triplicate cultures for each strain.

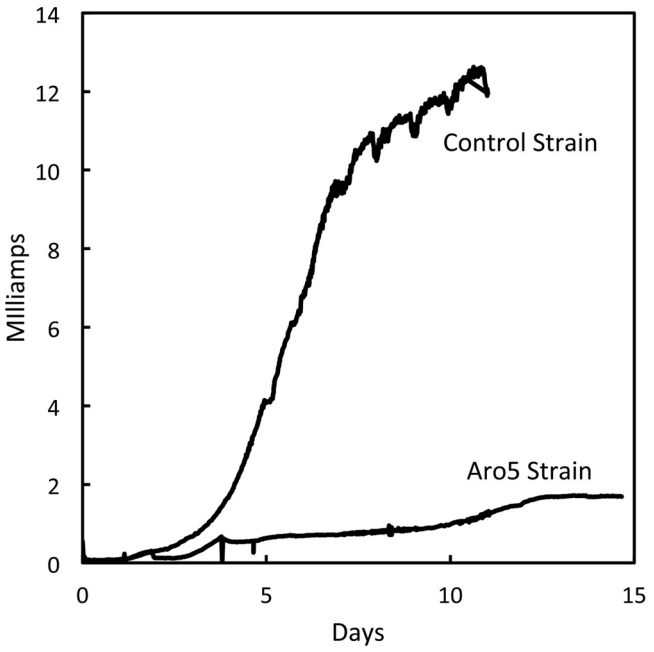

FIG 5 Current production in Aro-5 and the control strain, with acetate as an electron donor and anode poised at +300 mV versus Ag/AgCl. Results shown are representative of replicates.

The ability of Aro-5 to form relatively thick biofilms made it possible to measure the conductivity of Aro-5 biofilms in a previously described system (11) in which biofilms were grown on gold electrodes separated by a 50-μm nonconducting gap. The Aro-5 biofilms readily bridged the nonconducting gap (Fig. 7A), but the conductivity of the Aro-5 biofilm was 10-fold lower than that of the control strain (Fig. 7B).

Implications. These results suggest that the conductivity of *G. sulfurreducens* pili is a key feature in long-range electron transport. Even though the Aro-5 strain produced pili with properly localized OmcS, it was not capable of effective Fe(III) oxide reduction or high-density current production. The simplest explanation for these phenotypes is that the low conductivity of the Aro-5 strain pili prevents the long-range electron transport along the pili that is required for both of these types of extracellular electron transport.

The impact on conductivity of exchanging an alanine for the five aromatic amino acids in the carboxyl region of the *G. sulfurreducens* PilA sequence is consistent with the hypothesis that aromatic amino acids may account for the metallic-like conductivity of *G. sulfurreducens* pili (11), but in-depth structural studies, now under way, will be required to further evaluate this concept. The demonstration of a link between reduced pili conductivity and diminished capacity for long-range electron transport emphasizes the biological and environmental significance of such future structural investigations.

MATERIALS AND METHODS

Strains, plasmids, and culture conditions. Bacterial strains and plasmids used in this study are listed in Table S1 in the supplemental material. *G. sulfurreducens* strains were routinely cultured anaerobically (N_2-CO_2, 80:20) at 30°C in either acetate-fumarate or acetate-Fe(III) citrate medium, as previously described (22). For Fe(III) reduction studies, poorly crystalline Fe(III) oxide (100 mmol liter^{-1}) was the electron acceptor and Fe(II) in Fe(III)-reducing cultures was measured with the ferrozine assay (23). *Escherichia coli* was cultivated in Luria-Bertani medium with or without antibiotics (24).

Recombinant-strain construction. The wild-type allele of *G. sulfurreducens pilA* (locus tag GSU1496) was replaced on the chromosome with the mutant allele $pilA^{F53A,\ Y56A,\ Y61A,\ F80A,\ Y86A}$, designated $pilA^{Aro\text{-}5}$. A control strain was constructed by introducing the wild-type *pilA* sequence by the same methods. Structures of both the control and the mutant allele are described in Fig. 1. Primers used for construction of the control and $pilA^{Aro\text{-}5}$ allele are listed in Table S2 in the supplemental material. Briefly, the 3′ part of GSU1495 (0.5 kb) was amplified by PCR with primers GSU1495upBHI/GSU1495dnBHI, with *G. sulfurreducens* DL1 genomic DNA as the template. The resulting PCR product was digested with

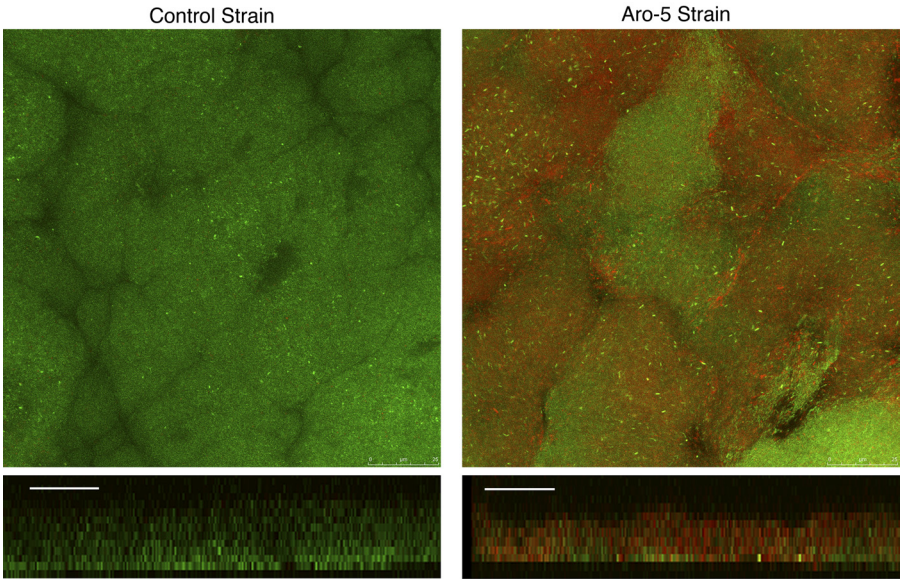

FIG 6 Confocal scanning laser micrographs of graphite anode biofilms of the control and Aro-5 strains. Top-down three-dimensional and horizontal side views (bottom images, anode) of cells stained with LIVE/DEAD BacLight viability stain. Bars = 25 μm.

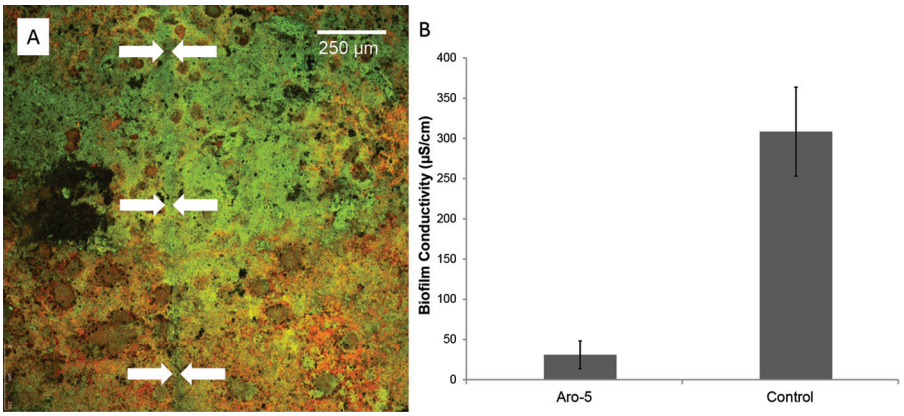

FIG 7 Properties of biofilms grown on gold anodes separated by a 50-μm nonconducting gap. (A) Confocal scanning laser micrograph of Aro-5 biofilm stained with LIVE/DEAD BacLight viability stain, demonstrating that the Aro-5 biofilms spanned the nonconducting gap. The position of the gap is designated by the white arrows. (B) Conductivity measured across the nonconducting gap for the control and Aro-5 strains (means ± standard deviations; $n = 3$ biofilms for each strain).

BamHI (New England Biolabs, Ipswich, MA, USA) and ligated with the T4 DNA ligase (New England Biolabs) upstream of the gentamicin resistance cassette into pCR2.1Gm^r*loxP* (25), resulting in plasmid pPLT173. P*pilA*, *pilA*, and the GSU1497 coding sequence (0.85 kb) were amplified by PCR with primers pilASNPUPXhoI/GSU1497SNPDNXhoI, with *G. sulfurreducens* DL1 genomic DNA as the template. The resulting PCR product was digested with XhoI and ligated with the T4 DNA ligase (New England Biolabs) downstream of the gentamicin resistance cassette into pPLT173, generating pPLT174. Mutations F53A, Y56A, Y61A, F80A, and Y86A were introduced into the *pilA* coding sequence with four rounds of mutagenic PCR with primers F53AY56A/F53AY56Ar, Y61A/Y61Ar, F80A-1/F80A-1r, and Y86A-1/Y86A-1r (Table S2) using the QuikChange Lightning site-directed mutagenesis kit (Agilent Technologies, Santa Clara, CA, USA), with pPLT174 as the template. The sequences of pPLT174 and pPLT174Aro-5 were verified by Sanger sequencing. The two plasmids were linearized with NcoI (NEB) and electroporated into *G. sulfurreducens* DL1 as previously described (22, 26). Recombinant strains were verified by PCR and Sanger sequencing.

RT-qPCR. Total RNA for real-time quantitative PCR (RT-qPCR) was extracted from triplicate cultures of wild-type DL1, DL1 Gent, and DL1 Aro-5 grown with acetate (15 mM)-fumarate (40 mM) during exponential phase at 25°C using the RNeasy minikit (Qiagen, Valencia, CA, USA) and treated with DNA-free DNase (Ambion, Austin, TX, USA). The RNA samples were tested for genomic DNA contamination by PCR amplification of the 16S rRNA gene (27). cDNA was generated with the TransPlex whole-transcriptome amplification kit (Sigma-Aldrich, St. Louis, MO, USA). The Power SYBR green PCR master mix (Applied Biosystems, Foster City, CA) and the ABI 7500 real-time PCR system were used to amplify and to quantify PCR products. Expression of *pilA* was normalized with that of *proC*, a gene shown to be constitutively expressed in *Geobacter* species (28). Relative levels of expression of *pilA* were calculated by the $2^{-\Delta\Delta C_T}$ method, where C_T is threshold cycle (29). Sequences from all primers used for RT-qPCR are listed in Table S2.

Immunogold labeling and transmission electron microscopy. The *c*-type cytochrome OmcS was localized with immunogold labeling as previously described (12). Late-log-phase cells that had been grown in a medium with acetate as the electron donor and fumarate as the electron acceptor were placed on 400-mesh carbon-coated copper grids for about 5 min. The samples were successively labeled with anti-OmcS rabbit polyclonal antibodies and anti-rabbit IgG conjugated with 10-nm gold-labeled secondary antibody, as previously described (12). Samples were then stained with 2% uranyl acetate and were observed using a Tecnai T12 electron microscope at an accelerating voltage of 100 kV. Images were taken digitally with a Teitz TCL camera system.

Pili conductivity. As previously described (11), for conductivity measurements, pili were sheared from the cells, and pili preparations (5 μg protein) were placed on split-gold electrodes and air-dried in a desiccator. In order to measure the pili conductivity under physiological conditions, a voltage ramp of 0 to 0.05 V was applied across split electrodes in steps of 0.025 V for 2-probe measurements using a source meter (Keithley 2400). For each measurement, after allowance for the exponential decay of the transient ionic current, the steady-state electronic current for each voltage was measured every second over a minimum period of 100 s using a LabVIEW data acquisition program (National Instruments). Time-averaged current for each applied voltage was calculated to create the current-voltage (I-V) characteristics.

Current production. The ability of the Aro-5 and control strains to couple the oxidation of acetate to electron transfer to positively poised graphite stick electrodes was determined in flowthrough bioelectrochemical systems as previously described (14).

Biofilm conductivity. As previously described (11, 13), biofilms were grown on arrays of four gold electrodes, each separated by a 50-μm nonconductive gap, in microbial fuel cells in which the electrodes served as the sole electron acceptor for acetate oxidation. To measure *in situ* biofilm conductivity, the gold anodes were disconnected from the cathode and connected to electronics. A source meter (Keithley 2400) was used to apply a fixed current between the outer of the four electrodes and to measure the potential drop between two inner electrodes (30), by measuring the voltage for each current every second over a period of 100 s, after the steady state was reached. An additional high-impedance voltmeter (Keithley 2000) was used to record the output voltage of the current source to calculate conductance (30).

As previously described (11), conformal mapping (31) was employed to calculate biofilm conductivity from measured biofilm conductance (G) according to following formula:

$$\sigma = G\frac{\pi}{L}/\ln\left(\frac{8g}{\pi a}\right)$$

where L is the length of the electrodes ($L = 2.54$ cm), a is the half-spacing between the electrodes ($2a = 50$ μm), and g is the biofilm thickness measured using confocal microscopy. This formula is valid for the limiting case $a < g \ll b$, where b is the half-width of the electrodes ($2b = 2.54$ cm).

The conductivity of pili preparations was calculated using the following relation (32):

$$\sigma = G\left(\frac{2a}{gL}\right)$$

Confocal microscopy. As previously described (18, 33), anode biofilms were imaged with confocal laser scanning microscopy using the LIVE/DEAD BacLight viability stain kit from Molecular Probes (Eugene, OR, USA), which contains two nucleic acid stains, the fluorescent green SYTO 9 stain and the fluorescent red propidium iodide. Images were processed and analyzed using the Leica LAS software (Leica).

SUPPLEMENTAL MATERIAL

Supplemental material for this article may be found at http://mbio.asm.org/lookup/suppl/doi:10.1128/mBio.00105-13/-/DCSupplemental.

Table S1, DOCX file, 0.1 MB.

Table S2, DOCX file, 0.1 MB.

ACKNOWLEDGMENTS

The information, data, and work presented herein were funded in part by Office of Naval Research Grants N00014-10-1-0084 and N00014-12-1-0229, and the Office of Science (Biological and Environmental Research), U.S. Department of Energy award number DE-SC0004114.

REFERENCES

1. **Lovley DR, Ueki T, Zhang T, Malvankar NS, Shrestha PM, Flanagan KA, Aklujkar M, Butler JE, Giloteaux L, Rotaru AE, Holmes DE, Franks AE, Orellana R, Risso C, Nevin KP.** 2011. *Geobacter*: the microbe electric's physiology, ecology, and practical applications. Adv. Microb. Physiol. **59**:1–100.
2. **Lovley DR.** 1991. Dissimilatory Fe(III) and Mn(IV) reduction. Microbiol. Rev. **55**:259–287.
3. **Lovley DR.** 1995. Microbial reduction of iron, manganese, and other metals. Adv. Agron. **54**:175–231.
4. **Lovley DR.** 2011. Live wires: direct extracellular electron exchange for bioenergy and the bioremediation of energy-related contamination. Energy Environ. Sci. **4**:4896–4906.
5. **Lovley DR.** 2012. Electromicrobiology. Annu. Rev. Microbol. **66**: 391–409.
6. **Summers ZM, Fogarty HE, Leang C, Franks AE, Malvankar NS, Lovley DR.** 2010. Direct exchange of electrons within aggregates of an evolved syntrophic coculture of anaerobic bacteria. Science **330**:1413–1415.
7. **Morita M, Malvankar NS, Franks AE, Summers ZM, Giloteaux L, Rotaru AE, Rotaru C, Lovley DR.** 2011. Potential for direct interspecies electron transfer in methanogenic wastewater digester aggregates. mBio **2**(4):e00159-11. http://dx.doi.org/10.1128/mBio.00159-11.
8. **Nevin KP, Lovley DR.** 2000. Lack of production of electron-shuttling compounds or solubilization of Fe(III) during reduction of insoluble Fe(III) oxide by *Geobacter metallireducens*. Appl. Environ. Microbiol. **66**: 2248–2251.
9. **Lovley DR.** 2012. Long-range electron transport to Fe(III) oxide via pili with metallic-like conductivity. Biochem. Soc. Trans. **40**:1186–1190.
10. **Reguera G, McCarthy KD, Mehta T, Nicoll JS, Tuominen MT, Lovley DR.** 2005. Extracellular electron transfer via microbial nanowires. Nature **435**:1098–1101.
11. **Malvankar NS, Vargas M, Nevin KP, Franks AE, Leang C, Kim BC, Inoue K, Mester T, Covalla SF, Johnson JP, Rotello VM, Tuominen MT, Lovley DR.** 2011. Tunable metallic-like conductivity in microbial nanowires networks. Nat. Nanotechnol. **6**:573–579.
12. **Leang C, Qian X, Mester T, Lovley DR.** 2010. Alignment of the *c*-type cytochrome OmcS along pili of *Geobacter sulfurreducens*. Appl. Environ. Microbiol. **76**:4080–4084.
13. **Malvankar NS, Tuominen MT, Lovley DR.** 2012. Lack of involvement of c-type cytochromes in long-range electron transport in microbial biofilms and nanowires. Energy Environ. Sci. **5**:8651–8659.
14. **Nevin KP, Kim BC, Glaven RH, Johnson JP, Woodard TL, Methé BA, Didonato RJ, Covalla SF, Franks AE, Liu A, Lovley DR.** 2009. Anode biofilm transcriptomics reveals outer surface components essential for high density current production in *Geobacter sulfurreducens* fuel cells. PLoS One **4**:e5628. http//dx.doi.org/10.1371/journal.pone.0005628.
15. **Reguera G, Nevin KP, Nicoll JS, Covalla SF, Woodard TL, Lovley DR.** 2006. Biofilm and nanowire production leads to increased current in *Geobacter sulfurreducens* fuel cells. Appl. Environ. Microbiol. **72**:7345–7348.
16. **Holmes DE, Chaudhuri SK, Nevin KP, Mehta T, Methé BA, Liu A, Ward JE, Woodard TL, Webster J, Lovley DR.** 2006. Microarray and genetic analysis of electron transfer to electrodes in *Geobacter sulfurreducens*. Environ. Microbiol. **8**:1805–1815.
17. **Franks AE, Glaven RH, Lovley DR.** 2012. Real-time spatial gene expression analysis within current-producing biofilms. ChemSusChem **5**:1092–1098.
18. **Franks AE, Nevin KP, Glaven RH, Lovley DR.** 2010. Microtoming coupled to microarray analysis to evaluate the spatial metabolic status of Geobacter sulfurreducens biofilms. ISME J. **4**:509–519.
19. **Snider RM, Strycharz-Glaven SM, Tsoi SD, Erickson JS, Tender LM.** 2012. Long-range electron transport in Geobacter sulfurreducens biofilms is redox gradient-driven. Proc. Natl. Acad. Sci. U. S. A. **109**:15467–15472.
20. **Malvankar NS, Lovley DR.** 2012. Microbial nanowires: a new paradigm for biological electron transfer and bioelectronics. ChemSusChem **5**:1039–1046.
21. **Craig L, Pique ME, Tainer JA.** 2004. Type IV pilus structure and bacterial pathogenicity. Nat. Rev. Microbiol. **2**:363–378.
22. **Coppi MV, Leang C, Sandler SJ, Lovley DR.** 2001. Development of a genetic system for *Geobacter sulfurreducens*. Appl. Environ. Microbiol. **67**:3180–3187.
23. **Lovley DR, Phillips EJ.** 1988. Novel mode of microbial energy metabolism: organic carbon oxidation coupled to dissimilatory reduction of iron or manganese. Appl. Environ. Microbiol. **54**:1472–1480.
24. **Sambrook J, Fritsch EF, Maniatis T.** 1989. Molecular cloning: a laboratory manual, 2nd ed. Cold Spring Harbor Laboratory Press, Cold Spring Harbor, NY.
25. **Aklujkar M, Lovley DR.** 2010. Interference with histidyl-tRNA synthetase by a CRISPR spacer sequence as a factor in the evolution of Pelobacter carbinolicus. BMC Evol. Biol. **10**:230. http://dx.doi.org/doi:10.1186/1471-2148-10-230.
26. **Lloyd JR, Leang C, Hodges-Myerson AL, Coppi MV, Cuifo S, Methe B, Sandler SJ, Lovley DR.** 2003. Biochemical and genetic characterization of PpcA, a periplasmic *c*-type cytochrome in *Geobacter sulfurreducens*. Biochem. J. **369**:153–161.
27. **Weisburg WG, Barns SM, Pelletier DA, Lane DJ.** 1991. 16S ribosomal DNA amplification for phylogenetic study. J. Bacteriol. **173**:697–703.
28. **Holmes DE, Nevin KP, O'Neil RA, Ward JE, Adams LA, Woodard TL, Vrionis HA, Lovley DR.** 2005. Potential for quantifying expression of the *Geobacteraceae* citrate synthase gene to assess the activity of *Geobacteraceae* in the subsurface and on current-harvesting electrodes. Appl. Environ. Microbiol. **71**:6870–6877.
29. **Livak KJ, Schmittgen TD.** 2001. Analysis of relative gene expression data using real-time quantitative PCR and the $2^{-\Delta\Delta C_T}$ method. Methods **25**: 402–408.
30. **Lange U, Mirsky VM.** 2008. Separated analysis of bulk and contact resistance of conducting polymers: comparison of simultaneous two- and four-point measurements with impedance measurements. J. Electroanal. Chem. **622**:246–251.
31. **Kankare J, Kupila EL.** 1992. In-situ conductance measurement during electropolymerization. J. Electroanal. Chem. **382**:167–181.
32. **Agrell H, Boschloo G, Hagfeldt A.** 2004. Conductivity studies of nanostructured TiO_2 films permeated with electrolyte. J. Phys. Chem. B **108**: 12388–12396.
33. **Nevin KP, Hensley SA, Franks AE, Summers ZM, Ou J, Woodard TL, Snoeyenbos-West OL, Lovley DR.** 2011. Electrosynthesis of organic compounds from carbon dioxide is catalyzed by a diversity of acetogenic microorganisms. Appl. Environ. Microbiol. **77**:2882–2886.
34. **Nunn DN, Lory S.** 1991. Product of the *Pseudomonas aeruginosa* gene *pilD* is a prepilin leader peptidase. Proc. Natl. Acad. Sci. U. S. A. **88**: 3281–3285.